Aero-Propulsive and Aero-Structural Design Integration of Turboprop Aircraft with Electric Wingtip-Mounted Propellers

van der Leer, Q.; Hoogreef, M.F.M.

DOI
10.2514/6.2022-0167

Publication date
2022

Document Version
Final published version

Published in
AIAA SCITECH 2022 Forum

AIAA SciTech Forum
January 3-7, 2022, San Diego, CA & Virtual
AIAA SCITECH 2022 Forum

10.2514/6.2022-0167

Aero-Propulsive and Aero-Structural Design Integration of Turboprop Aircraft with Electric Wingtip-Mounted Propellers

Quinty van der Leer*, Maurice F. M. Hoogreef†
Delft University of Technology, Delft, 2600AA, The Netherlands

The current focus in the aviation industry for more sustainable designs, could mean the revive of propeller propulsion, due to their relative high propulsion efficiency compared to jets. In addition, wingtip-mounted propellers installed in tractor configuration can be used as tip-vortex attenuating devices, reducing the wing induced drag. So far, studies on wingtip-mounted propellers mainly concentrated on the aerodynamic interaction effects, disregarding the integration with the airframe and wing-structural mass. This paper presents a method to integrate into an aircraft sizing process the aerodynamic, aero-propulsive, and aero-structural effects of tip-mounted propellers, in the context of a typical turboprop featuring hybrid-electric propulsion. Subsequently, a number of case studies are performed to investigate the sensitivity to modifications of the propulsion system on wing and aircraft level. Results show that the performance benefit gained by the application of a wingtip-mounted propeller is easily overruled by the weight penalty that it introduces, an almost linear relationship between shaft power ratio φ and MTOM was observed. For variations of propeller diameter, it is seen possible to attain equal performance in terms of energy efficiency with a mass penalty. For $\varphi = 0.1$, the reference performance is obtained for a tip-mounted propeller occupied span fraction of $\Delta Y = 0.175$ with an increase in MTOM of 2.8%. For $\varphi = 0.2$, this is obtained at a larger tip-mounted propeller ($\Delta Y = 0.275$) and an increase in MTOM of 5% compared to the reference design.

Nomenclature

Latin symbols

A_R	=	Disk area ratio (m^2)
B_p	=	Number of blades per propeller(∼)
b	=	Span(m)
C_L	=	Lift coefficient (∼)
C_D	=	Drag coefficient (∼)
D_p	=	Propeller diameter(ft)
E	=	Energy (J)
G	=	Jet correction (∼)
k_p	=	Propeller mass coefficient (∼)
M	=	Mach number (∼)
m	=	Mass (lbs)
N_p	=	Numper of propellers (∼)
P_s	=	Shaft power (W)
P_{to}	=	Take-off power (hp)
R	=	Radius (m)
R	=	Range (km)
U_j	=	Jet velocity (m/s)
W	=	Weight (N)

Greek Symbols

η	=	Propeller spanwise location
Γ	=	Circulation
μ	=	Velocity ratio
φ	=	Shaft power ratio

Subscripts

alt	=	Altitude
ib	=	Inboard
wt	=	Wingtip

Abbreviations

AIC	=	Aerodynamic Influence Coefficient
APS	=	Aero-Propulsive and Aero-Structural
AVL	=	Athena Vortex Lattice
BEM	=	Blade Element Method
DHEP	=	Distributed Hybrid Electric Propulsion
FEM	=	Finite Element Method
MTOM	=	Maximum Take-Off Mass
PREE	=	Payload Range Energy Efficiency
PTE	=	Partial Turbo Electric
VLM	=	Vortex Lattice Method
WTMP	=	WingTip-Mounted Propeller
ZFM	=	Zero Fuel Mass

*MSc. Student, Faculty of Aerospace Engineering, Delft University of Technology, P.O. Box 5058, 2600 GB Delft, The Netherlands
†Assistant Professor, Faculty of Aerospace Engineering, Delft University of Technology, P.O. Box 5058, 2600 GB Delft, The Netherlands, AIAA Member

I. Introduction

Due to the rising concern about climate change, the aviation industry is forced to look into more environmental friendly solutions and design concepts. A shift towards more propulsive efficient designs is required. Propellers are an attractive option since they have a relative high propulsive efficiency compared to jets. Moreover, when correctly integrated with the wing, their mutual interaction offers aerodynamics benefits. Already in the 1980's, aerodynamic studies [1][2] showed that a correct integration of wing and propeller can result in a significant performance increase. Besides providing propulsion, propellers can be used to attenuate the tip vortex. Miranda and Brennan [2] studied two different ways to achieve this tip vortex attenuation: a pusher propeller and a tractor propeller at the wingtip. It was found that both configurations lead to a reduction in required power. The performance benefit of a pusher propeller occurred through increased propeller efficiency whereas the tractor propeller resulted in decreasing induced drag.

Wingtip-mounted propellers in tractor configuration are believed to reduce the wing induced drag significantly, this was derived from both experimental [3, 4] and numerical studies [2, 5]. All of these studies stress the importance of the sense of rotation of the propeller which has to counteract the wingtip vortex, resulting in an inboard-up rotation. In this manner, the propeller swirl attenuates the tip vortex and reduces the corresponding tip-losses.

The introduction of Hybrid Electric Propulsion (HEP) offers more design freedom and makes the use of distributed propulsion more attractable [6]. This could enable the use of a wingtip-mounted propeller next to an inboard situated propeller in a hybrid electric power train. The wingtip-mounted propeller will provide an induced drag reduction and simultaneously be responsible for part of the total thrust provided by the propulsors. This results in the ability to downscale the inboard propeller. This down scaling, possible re-positioning and application of the wingtip propeller will all influence the lift distribution and change the inertia loads on the wing. The wingtip-mounted propeller configuration both impacts the aerodynamics and structures of the system.

Ultimately, these disciplines need to be coupled in order to assess the wingtip-mounted propeller potential on a higher level. Numerous integration studies have been performed on (variations of) wingtip-mounted propeller configurations. Some studies have mainly investigated the aerodynamic effects [7–10]. Some studied the effect on the aircraft weight by assuming aerodynamic benefits [11] or by ignoring mutual interference [12]. Others integrated both aerodynamic and structural disciplines but used simplified surrogate models for aero-propulsive effects and assumed a clean wing for the aerodynamic load used for the structural wing weight estimation [13].

The inclusion of the wingtip-mounted propeller has an effect on the aerodynamic load distribution and alters the distribution of the inertia loads on the wing. So far, none of the studies attempted a complete integration of aerodynamic, propulsive and structural effects of a wingtip-mounted propeller configuration. In this paper, a methodology is presented to investigate the potential of the wingtip-mounted configuration when aero-propulsive and (aero-)structural effects are accounted for. This methodology is used to assess whether performance benefits of a wingtip-mounted propeller configuration are still substantial when not only looking at aero-propulsive but also at structural effects.

The study focuses on a typical turboprop aircraft with two additional wingtip-mounted propellers. The aircraft features a Partial Turbo Electric (PTE) power train where the wingtip-mounted propellers are driven by electric motors. The configuration is illustrated in Figure 1. The coupled effect of the integrated aerodynamic, propulsive and structural effects of wingtip-mounted propellers on aircraft performance is investigated on both wing and aircraft level.

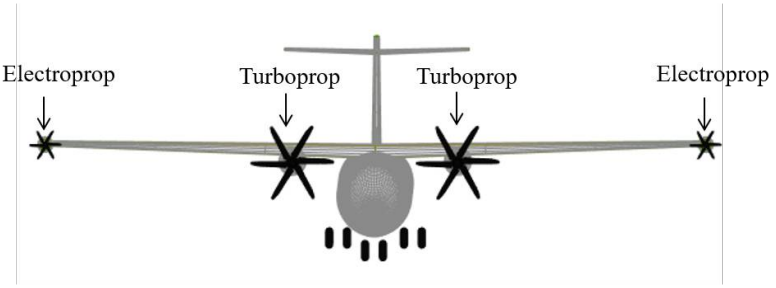

Fig. 1 Front view of a wingtip-mounted propeller configuration as studied in this paper

An aero-propulsive model is developed to determine the aerodynamic loading and performance of propeller-wing systems at different flight conditions. This model is integrated within an aero-structural model providing aerodynamic wing loading for the structural sizing conditions. The aero-propulsive and aero-structural models are discussed in

Section II. Here, the integration on wing and aircraft level is discussed as well. The validity of the models is shown in Section III. The different case studies and their results are presented in Sections IV and V respectively.

II. Methodology

The methodology consists of two main parts. An aero-propulsive model that couples the wing and propeller aerodynamics, and an aero-structural model that couples the aerodynamics to the structural wing weight. These two models are combined to inter-relate the aerodynamics, structures and propulsion of the system inside a conceptual aircraft design framework to include aircraft sizing effects.

A. Aero-Propulsive Model

The aero-propulsive model is based on the work performed by Willemsen [14]. He developed a numerical method to study the mutual aerodynamic interaction between the wing and a wingtip-mounted propeller in tractor configuration. This method has been extended such that it could be used for a wing featuring both a wingtip-mounted and main propeller.

The numerical method consists of a propeller and wing model. A Blade Element Method (BEM) analyses the performance of the propeller and is used to generate a performance map. This map is utilized in the performance analyses for a propeller in a non-uniform inflow field that is adopted from van Arnhem et al. [15]. A tractor propeller experiences a non-uniform inflow, as the velocity field is disturbed by the presence of the wing. Similarly, the velocity field experienced by the wing is modified by the propellers presence. To evaluate the propeller induced velocity field, an extended version of the slipstream model by Conway [16] is used. The enhancement meant that also slipstream contraction, deflection and the azimuthal circulation distribution are accounted for.

The aerodynamic wing model includes a Vortex Lattice Method (VLM) and is able to cope with a non-uniform inflow field as imposed by the propeller. The model enclosed a jet correction to account for the finite height of the propeller slipstream. A Trefftz plane analysis is used to calculate the wing induced drag. When 2D airfoil polars are included, viscous effect can also be account for. The lift is corrected by a correction applied to the angle of attack for every single vortex strip. The way the viscous lift correction is determined is visualized in Figure 2. Thin airfoil theory is conventionally used in vortex lattice methods. The viscous polars can be obtained by Xfoil * for example. These can also be used to determine the skin friction coefficient. The wing model eventually yields a loading distribution as well as the wing induced velocity field.

There is a mutual interaction between the wing and the propeller. The performance of the wing depends on the propeller induced velocities, while the propeller itself depends on the wing induced velocities. For this reason, the propeller-wing system aerodynamic analyses requires an iterative procedure. This process flow is depicted in Figure 3.

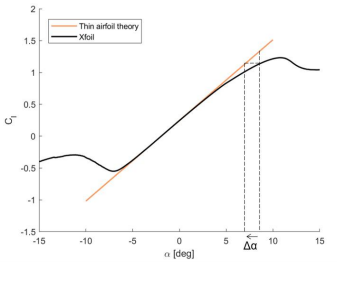

Fig. 2 Visualisation of the way the viscous correction is determined

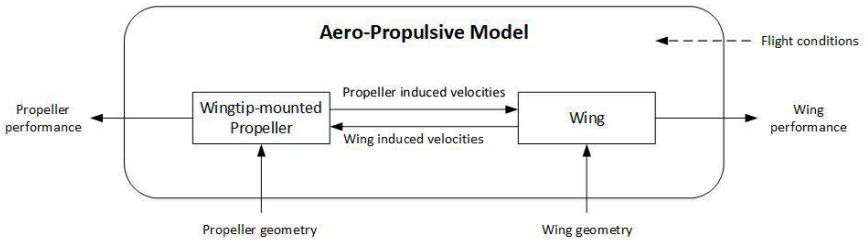

Fig. 3 Flow chart of unmodified aero-propulsive model

An important feature of the wing model is that it includes a correction for the finite height of the propeller slipstream. An airfoil immersed in a slipstream with jet velocity U_j and a finite radius R, produces less lift than an airfoil experiencing a freestream velocity of U_j. This effect is mainly present for the axial velocity direction and can be neglected for the tangential direction [17]. Rethorst [18] developed a method to account for the effect of the finite height of the slipstream. He introduced a correction matrix to be applied to the Aerodynamic Influence Coefficient (AIC) matrix.

*https://web.mit.edu/drela/Public/web/xfoil

The correction is based on pressure and slipstream continuity on the jet boundary. Although the method was developed for a propeller on the wing symmetry axis, it can also be applied to an asymmetrical configuration since the correction is most noticeable around the jet boundary [17]. In order to apply it to an asymmetric case, an imaginary wing part needs to be introduced. This imaginary wing part ensures the propeller to be in the centre of the wing as shown in Figure 4. For this example, the jet correction will be calculated for section I. The correction for sections II and III are obtained by mirroring the correction matrix of section I. The correction obtained for section III will be disregarded because this is only an imaginary wing section. It must be noted that this correction imposes a number of conditions for the VLM mesh used. First of all the jet centerline must be in the center of one the vlm strips and the jet boundary must coincide with one of the strip boundaries. Moreover, the distribution of the vortex strips should be symmetric about the propeller axis. For the wingtip-mounted propeller this does not impose any problems as the symmetry section only consists of a virtual wing part and will be disregarded.

The jet correction as described by Rethorst [18] assumed the propeller slipstream to be uniform in axial direction. In reality, a propeller introduces a distribution in axial velocity in the slipstream. The assumption has been revised and modified by Willemsen [14] to the assumption of a radially symmetric axial velocity distribution. The jet velocity is discretized and for every significant step in velocity μ_i, a correction matrix G_i is calculated as if a jet with of radius r_i and axial induced velocity u_i is present. Summing all the correction matrices results in the total jet correction to be applied. This approach is visualised in Figure 5.

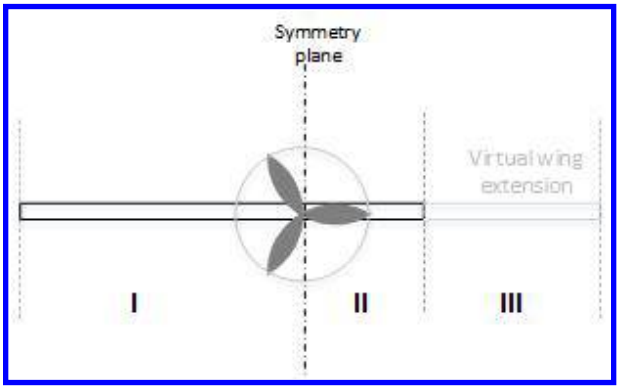

Fig. 4 Example of propeller-wing system for jet-correction.

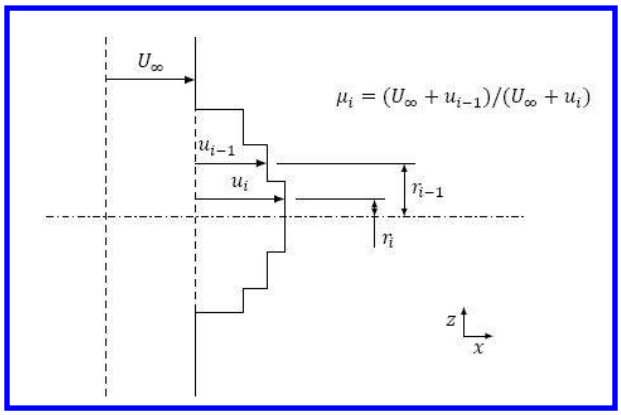

Fig. 5 Discretization of a jet velocity profile for the calculation of the jet correction [14]

The aforementioned model has been adapted such that it could analyse propeller-wing systems of interest for this study. This means that it is able to analyse a wing with a wingtip-mounted propeller and a main propeller in tractor configuration. Moreover, it is suitable for a regional turboprop in terms of aircraft dimensions and flight conditions.

The major modification is the addition of an additional propeller. To combine two propellers on one wing-half, it is assumed that the propellers do not have an effect on each other. It was found that both the axial and tangential propeller induced velocities rapidly approaches zero once the distance to propeller axis is larger than its radius, as sketched in Figure 6. Since both propellers will be much farther apart for the case studies considered here, this assumption holds. This also means that the induced velocities by the propeller can simply be superimposed onto the wing velocity field. An updated process flow of the aero-propulsive model is shown in Figure 7.

The original jet correction was only valid for a wingtip-mounted propeller. Its formulation has been modified to make it applicable to propellers at arbitrary spanwise location. As mentioned before, the jet correction assumes propellers to be located at a (virtual) symmetry axis of the wing. It requires VLM strips to be distributed symmetrically about the propeller axis. Naturally, the wing root also needs to be an axis of symmetry since the propulsion system is symmetric around the centerline. Figure 8 shows the symmetry axes required for a propeller wing system with two main propellers.

Obeying these symmetry requirements, the jet correction matrix can be generated in two different ways. The correction can be calculated for one wing half first. This means calculating the correction for section I-A, mirroring about I with the other wing side as imaginary. Subsequently, the correction matrix can be mirrored to obtain the correction for the other wing half. Alternatively, the correction can be calculated for the complete wing (section A-B) with one propeller first and its inverse can be added to the matrix to obtain the correction for a complete wing with two

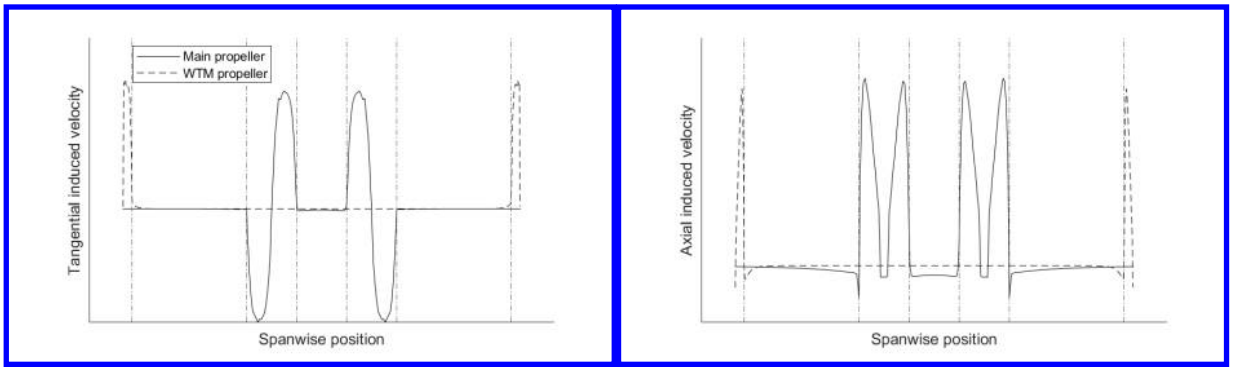

(a) Tangential induced velocity (b) Axial induced velocity

Fig. 6 Illustration of typical tangential and axial induced velocity distribution over the wing with inboard and tip-mounted propeller

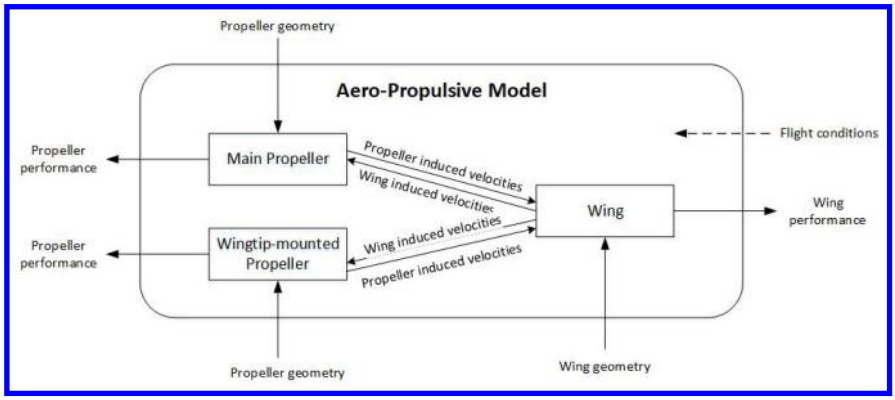

Fig. 7 Flow chart of modified aero-propulsive model

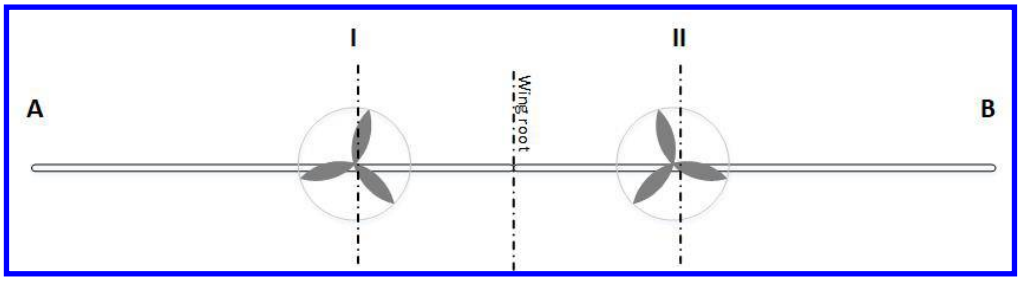

Fig. 8 Symmetry axes required for jet correction due to main wing.

main propellers. Again, these tricks can be applied because the correction is most present around the jet boundary. This also enables the superposition of the obtained correction matrices for the inboard and wingtip-mounted propeller.

For an inboard propeller, the first method is preferred because the second method can only be applied if a uniform strip distribution is used which is far from desired. Consequently, for a wing with a wingtip-mounted propeller and inboard propeller, the wing mesh will need to be divided into five sections as shown in Figure 9. Section I and III need to have the same amount of strips and a similar, but opposite, spacing (eg. inverse sine vs sine). Section II needs an uneven number of strips and a symmetric spacing about its centre. The type of spacing used per section is shown in Table 1. A convergence study has been performed to determine the optimum number of panels regarding computational time and accuracy.

The original aero-propulsive model was only used for low flight speeds and no mach number correction was included

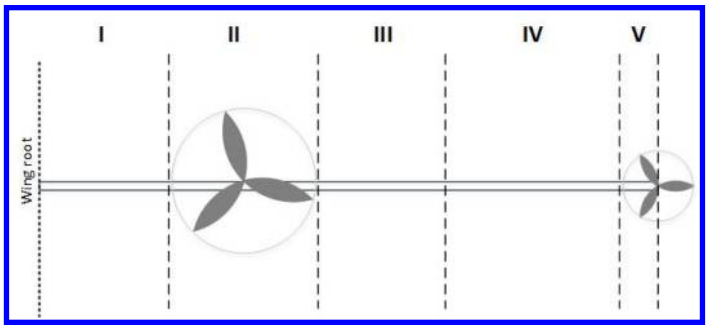

Fig. 9 Division of wing sections.

Table 1 Type of spacing used per section.

Section	I	II	III	IV	V
Spacing	Inverse sine	Uniform	Sine	Inverse sine	Uniform

in the wing model. As a turboprop aircraft is to be studied at cruise conditions and varying flight speeds (M= 0.5-0.6), compressibility effect will become more significant. That is why a Prandtl Glauert compressibility correction has been applied to the vortex strength at each panel. This means that the corrected circulation is given by $\Gamma_c = \frac{1}{\sqrt{1-M^2}}\Gamma_i$.

B. Aero-Structural Model

Besides the wing layout and inertia loads, the aero-structural model uses the aerodynamic loading on the wing to estimate the wing mass. These calculations should be performed at the flight condition that sizes the wing mass. For this, a 2.5G pull up is used at M_{cruise}†1.05 and $alt_{cruise} + 3000ft$ with both Maximum Take-Off Mass (MTOM) and Zero Fuel Mass (ZFM). As the flight conditions and operating weight are know, the required lift coefficient is easily deducted by the lift formula. AVL [†] is used to get the approximate division of lift between the wing and horizontal tail and the required angle of attack. The inviscid propeller-wing model is analysed at this angle of attack with propeller power at cruise settings and yields the aerodynamic load distribution over the wing. This loading distribution is scaled to match the required wing lift coefficient and is forwarded to the structural model together with the known wing geometry and engine specifications. An overview of the process flow of the aero-structural model is shown in Figure 10.

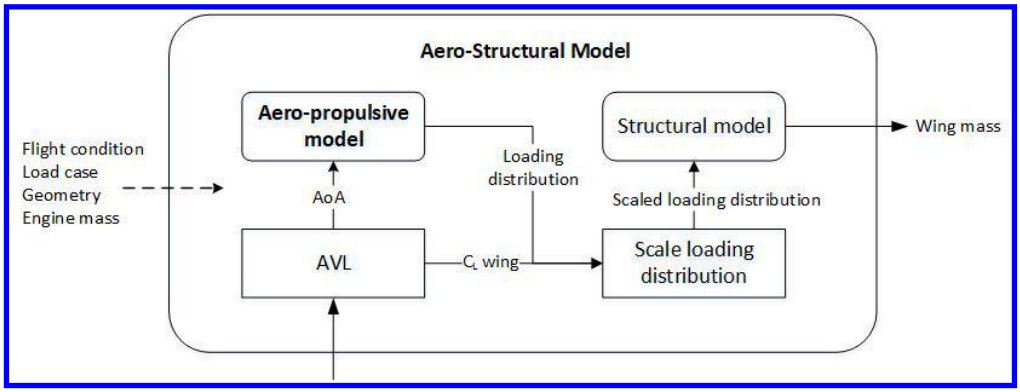

Fig. 10 Overview of aero-structural process flow.

The structural model consist of a Finite Element Method (FEM) developed by Elmendorp and La Rocca [19]. It discretises the wing and uses an idealised boom representation to model the wing sections as, for example, described in Megson [20]. It optimises the wing box design in order to get the minimum amount of primary structure required. Nevertheless, it should withstand the critical loadcase without exceeding the maximum allowable mechanical stress in

[†] http://web.mit.edu/drela/Public/web/avl/

the structural members, with a 1.5 safety factor included. The weight of the secondary elements is based on the weight of the wingbox and is estimated using the method by Torenbeek [21].

The structural wing weight estimation is sensitive to the aerodynamic load, consisting of lift, drag and moment distribution. It also takes the weight of the engines into account. These are included as discrete loads on the wing.

C. Aero-Propulsive-Structural Integration

The aero-propulsive and aero-structural models are coupled to be able to study the effect of a change in configuration on a broader level than just focusing on one of the two disciplines. In order to have the required information available on the design, a sizing procedure is required. The sizing methodology used for wing and aircraft level are discussed below.

1. Wing Level

On wing level, the impact of the propulsion system on the wing mass is studied by use of a reference design. The wing design and propeller design itself are kept constant and only the propulsive design is modified in terms of shaft power ratio, disk area ratio, and location. The change in propulsive design affects the structural wing weight in two ways. It alters the aerodynamic loading distribution on the wing and it changes the distribution of the engines masses over the wing. The changes in engine mass are estimated by an engine sizing procedure. This also determines the individual propeller rotational velocity to produce the required thrust. An overview of the propulsion system sizing procedure is shown in Figure 11. The method uses the following assumptions:

- The total shaft power remains constant
- The shaft power ratio equals the thrust split
- The total required thrust is not affected by the design modifications
- The total disk area remains constant
- The axial distance between the wing leading edge and propeller remains constant
- The propeller offset in vertical direction is normalised by the radius and remains constant
- MTOM is assumed unaffected

The total disk area is the total area of the propellers combined. It is kept constant to be able to vary the individual disk loading of the propellers while maintaining a constant total disk loading. Not all propulsive design modifications are feasible. The design is limited by the tip Mach number of the propellers and the available power of the engines. Moreover, if the specified main propeller location and dimension results in contact with the fuselage, the design is disregarded. The outboard placement of the main propeller is also limited by the imposed VLM grid constraints.

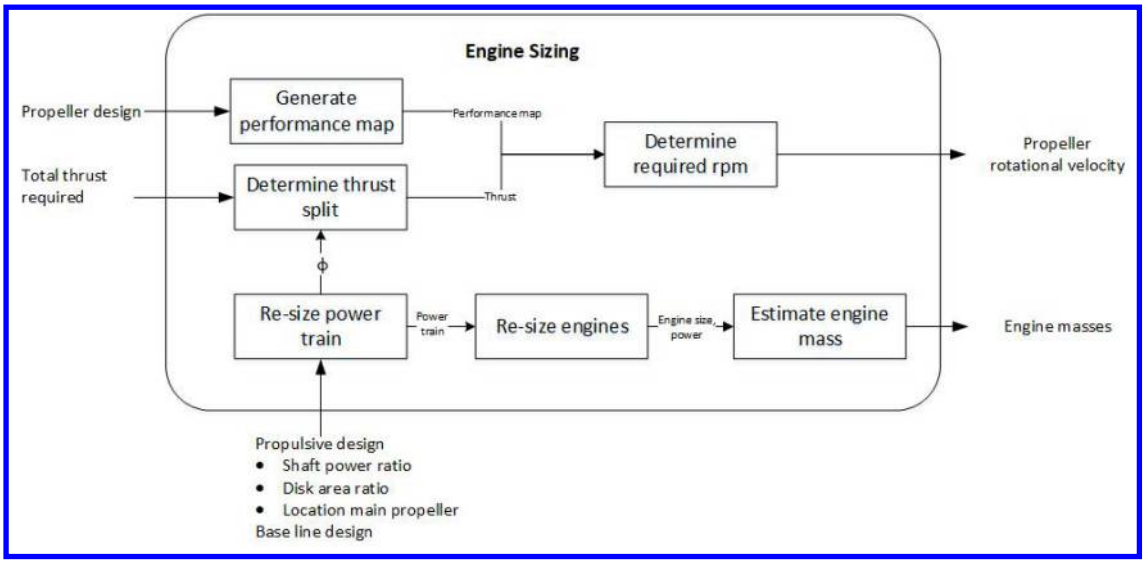

Fig. 11 Overview of engine sizing process flow.

2. Aircraft Level

For the aircraft level study, the aero-propulsive and aero-structural models are coupled and included within a design convergence loop. The in-house developed conceptual design tool, the Aircraft Design Initiator (or in short the *Initiator*), is used for this. The initiator performs a design convergence over a number of disciplinary analyses and sizing methods. The work of de Vries et al. [22] on preliminary sizing methods for DHEP made it possible to synthesize hybrid electric aircraft configurations. Additionally, a simplified surrogate model was included to quantify the effects of distributed propulsion on the wing aerodynamics. More information on the initiator can be found in [13, 23, 24].

The aero-propulsive and aero-structural models are integrated in the Class II.V method of the Initiator as shown in Figure 12. At this point in the convergence process, the aircraft geometry is available and the weight results of the Class I and Class II methods have already converged. Placing the models within this Class II.V method avoids the aero-propulsive analyses to be run in the early stage of the design loop. The wing weight estimation uses the loading distribution obtained by the aero-propulsive analysis at the critical condition to account for the propulsive effects on the wing structural weight. The wing weight is used to update the MTOM. In addition, the aero-propulsive model is ran for the cruising condition to get better estimate of the effects of the propellers on the wing performance in cruise. This effect is quantified in terms of ΔC_L and ΔC_D and is feed forward to the Class I mission analyses in the next iteration and is used instead of the surrogate model.

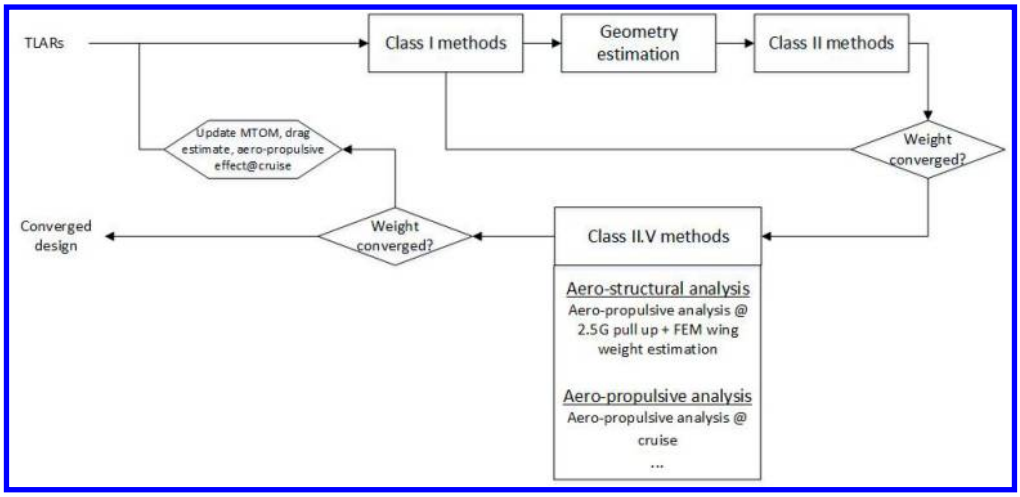

Fig. 12 Simple overview of the updated initiator process flow.

The integration of the aero-propulsive and aero-structural effects within the Initiator makes it possible to study the effects of these interdisciplinary interactions on aircraft level as a converged design is formed.

The Class II weight estimation method by Torenbeek [21] has been slightly modified in terms of the propeller weight estimation. Using the same regressions parameters as originally used by Torenbeek, new coefficients were determined for more modern propellers as the original would significantly overestimate masses of modern propellers. To this end, a regression was constructed through data obtained from type-certificate datasheets. The resulting equation is much more accurate for modern composite propellers whereas the original is better suited to aluminium propellers. With more reference data and for example only composite propellers, the coefficients could still be further refined. The original equation is shown in (1); the modified in (2); here k_p is 0.108 for imperial units in the equation as specified in [21], N_p is the number of propellers, D_p is propeller diameter in feet, B_p the number of blades per propeller and P_to the take-off power in horse-power, resulting mass is in pounds.

$$m_{\mathrm{prop}_{installation}} = k_\mathrm{p} \cdot N_\mathrm{p}\left(D_\mathrm{p} \cdot P_\mathrm{to} \cdot \sqrt{B_\mathrm{p}}\right)^{0.78174} \tag{1}$$

$$m_{\mathrm{prop}_{installation}} = k_\mathrm{p} \cdot N_\mathrm{p}\left(D_\mathrm{p} \cdot \sqrt{B_\mathrm{p}}\right)^{0.85} \cdot {P_\mathrm{to}}^{0.67} \tag{2}$$

III. Validation

The individual unaltered methods have been validated before. More information on this can be found in the respective research. For this reason, this section will focus on the adaptions made to the models and their integration.

A. Aerodynamic

In terms of the wing aerodynamics, a compressibility correction has been added and a method to determine the pitching moment distribution has been introduced. The results obtained for the modified method are compared to analyses by AVL (itself also a vortex lattice method). A clean wing (no propellers) was used. Furthermore the wing is tapered, swept and uses an asymmetric airfoil. The geometry used is representative for a wing of interest in this study. The results are shown in Figure 13. It can be seen that the lift distribution matches quite well while the moment distribution shows some discrepancies. A constant offset between the AVL and modified VLM (in all figures indicated simply as VLM) predicted moment is observed across the span. This is caused by the fact that currently the wing model only accounts for the pitching moment caused the lift and disregards the moment introduced by the airfoil camber. The effect of this discrepancy on the wing weight has been investigated and it was found that the structural model is relatively insensitive to the magnitude of the pitching moment distribution. The wing weight was determined for various designs both using the pitching moments distribution computed by AVL and modified VLM. The results showed that the difference in pitching moment leads to a difference of wing mass of 2kg maximum, which is insignificant.

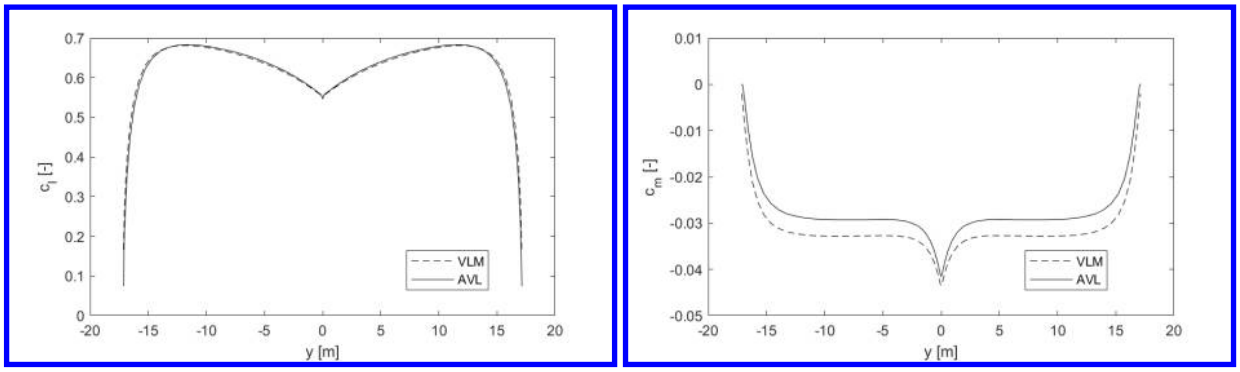

(a) Lift distribution

(b) Pitching moment distribution

Fig. 13 Comparison of load distribution computed by AVL and modified VLM for a clean aerodynamic wing

B. Aero-Propulsive

The original aero-propulsive method was build for a wing with a wingtip-mounted propeller only. Willemsen [14] checked its validity by comparing the method's results against experimental data collected by Sinnige et al. [4]. For completeness, the comparisons of the predicted aerodynamic polars for the wing with a wingtip-mounted propeller are shown in Figure 14(a) and 14(c).

The same experiment was performed for an inboard propeller. This data has been used to validate the correct implementation of the inboard propeller in the aero-propulsive model. The results are shown in Figure 14(b) and 14(d). Both numerical and experimental data show that the lift increases with a decrease in advance ratio (which equals a thrust increase). Moreover, the validation data shows an increase in lift curve slope for increasing thrust. This trend is also predicted by the numerical model. The two configurations also show similar behaviour in terms of the numerical predicted lift-drag polar compared to the experimental data. Two sources of discrepancies wing and propeller model In general, the aero-propulsive model is able to model the major trends of the interfering propeller-wing system.

C. Aero-Structural

The aero-structural model has the aero-propulsive model integrated within it to get the aerodynamic loading distribution. Originally, the structural used AVL to get this distribution. To check whether the aerodynamic model is correctly integrated, the results obtained by using AVL and a clean aerodynamic wing have been compared. This has been done for a number of design modifications and different starting points. Figure 15(a) shows that both methods

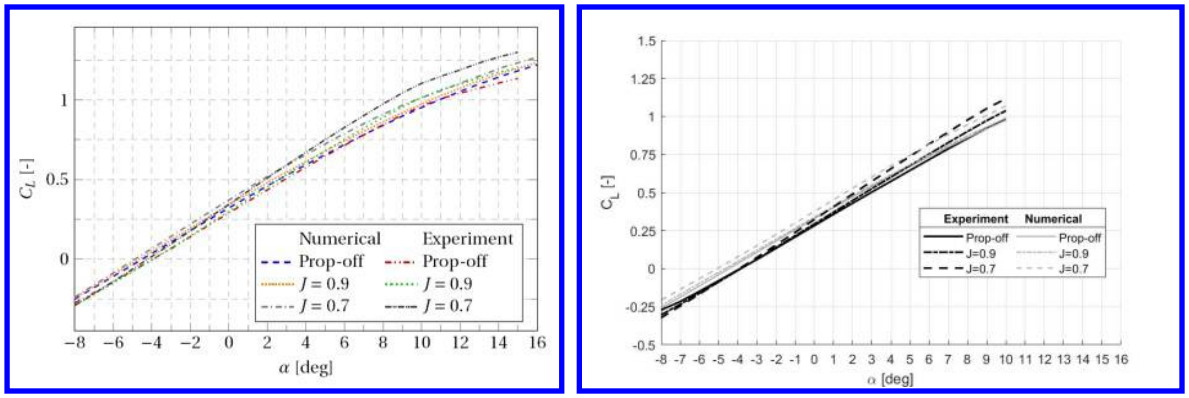

(a) Lift polar- Wingtip propeller only [14]

(b) Lift polar - inboard propeller only

(c) Lift drag polar - wingtip propeller only [14]

(d) Lift drag polar - inboard propeller only

Fig. 14 Comparison of numerical results of the aero-propulsive model with experimental results [4]

show the same sensitivity to a design modification. For the same design modification both methods predict an equally large change in wingmass compared to the baseline design. The absolute difference between the wingmass obtained by both methods is in the order of 0.5% as shown in Figure 15(b). Overall, the integration of the aero-propulsive model within the structural analyses performs as desired.

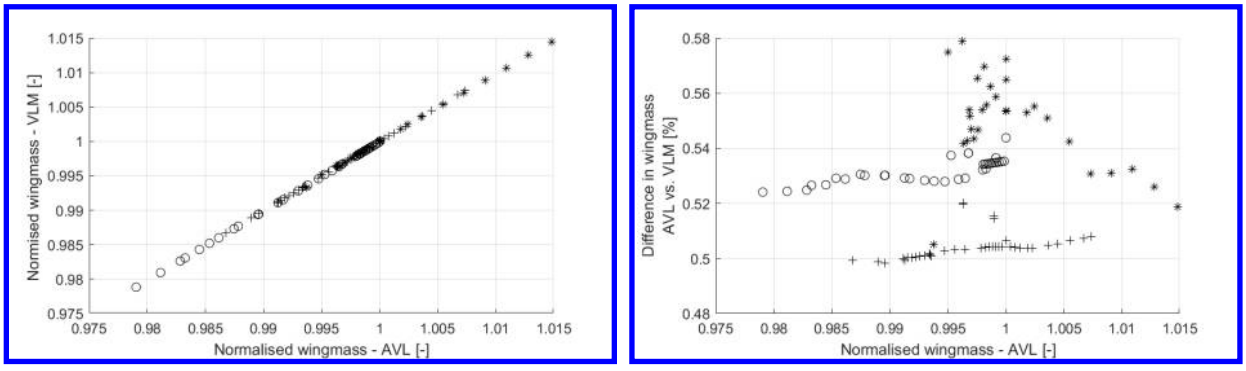

(a) Normalised wingmass

(b) Difference in wingmass

Fig. 15 Wingmass comparison for different design by using AVL and modified VLM predicted loading distributions for a clean aerodynamic wing.

IV. Case Study

A. Reference Aircraft

The designs studied are all based on the wingtip-mounted propeller configuration with a high technology level assumed as studied by Hoogreef et al. [13]. The high technology level assumes an Equivalent Specific Power (ESP) of 9.1 kW/kg for the electrical machines and a Specific Power (SP) of 10.5 kW/kg for the gas turbine. The ESP is a measure for combined specific power and is introduced in de Vries et al. [25]. The top level requirements of the reference are presented in Table 2.

Table 2 Top level requirements for reference aircraft

Spec	Unit	
Harmonic range	km	2037
Structural payload	kg	15000
Passengers	-	150
Cruise Mach	-	0.6
Cruise altitude	m	7620
Take-off distance	m	2200
Approach speed	m/s	71

As the developed aero-propulsive model cannot cope with varying wing thicknesses or kinks in the wing planform, the design has been slightly modified such that the aero-propulsive model could be used. The kink has been removed and in terms of the wing airfoil, the ATR72 Smoothed Airfoil[2] [‡] with 18% thickness has been used. An isometric view of the resulting reference design in conventional configuration is shown in Figure 16. It is important to mention that these modifications have a substantial influence on resulting design in terms of performance. It leads to an increase of 5% in MTOM and a reduced PREE of 12%. This is mainly caused by the constant thickness of the airfoil along the span, resulting in a relative high thickness at the tip. Nevertheless, this does not pose an issue for relative comparison between designs.

Fig. 16 Isometric view of the conventional reference design

B. Wing Weight Sensitivity

To study the wing weight response to the wingtip-mounted propeller system configuration, a baseline design with predefined shaft power ratio is used. This is a converged PTE wingtip-mounted propeller configuration design. The wing design is kept constant while the parameters listed in Table 3 are varied. The last listed parameter varies the shaft power ratio and disk area ratio simultaneously such that the individual disk loading of the propellers remain unchanged. The shaft power ratio indicates the power of the secondary shaft over the total shaft power. The area ratio is defined as the main disk area divided by the total disk area.

The propulsive design affects the load on the structure by its aero-propulsive load and by a modified discrete load due to a change in the propulsion system mass. In order to examine the contribution of both, the sensitivity study is

[‡] `http://airfoiltools.com/airfoil/details?airfoil=atr72sm-il` [Accessed: 08-07-2020]

performed for an aerodynamically clean wing and full-interaction propeller-wing system. The first approach isolates the effect of the mass of the engines, whereas the second approach includes both the aerodynamic and discrete load.

Table 3 Design modifications for the wing weight sensitivity study

Parameter	Range	Baseline (φ=0.2)
Power ratio, φ	0.1-0.35	0.2
Main propeller location, η	0.25-0.3	0.25
Disk area ratio, A_R	0.764-0.983	0.874
Power ratio (with constant individual disk area), φ	0.1-0.35	0.2

C. Aircraft Level Sensitivity

To quantify the sensitivity of the aircraft design to the PTE power split, the reference design has been modified in terms of shaft power ratio. Shaft power ratios of 0.1, 0.2 and 0.3 are used. These configurations are synthesised using the Initiator with and without the integrated aero-propulsive and aero-structural (APS) models included. The converged designs are compared to the reference aircraft in terms of MTOM, wing weight, propulsion system weight and PREE in order to asses the effect of the wingtip-mounted propeller configurations on aircraft level performance. In addition, two other designs configurations have been synthesised. A wingtip-mounted propeller-only design and a wingtip-mounted propeller design with a conventional configuration using two turboprops instead of one turboprop and one electroprop.

V. Results

This section discusses the results for both the wing and aircraft level sensitivity studies performed.

A. Wing Weight

On wing-propulsion level, over 200 design points were evaluated, divided over 3 baseline designs with initial shaft power ratios of 0.1, 0.2 and 0.3. All three baseline studies showed similar results, confirming the sensitivity of the analysis. It should be noted that this approach purely studies the effect of a change in propulsion system design on the wing weight. The wing design is unmodified and there is no feedback to the higher-level aircraft design in terms of mass or performance.

An overview of the results for the baseline design with a shaft power ratio of 0.2 are presented in Figure 17. The marker shades indicate an increase or decrease of the varied parameter compared to the reference value. Results are shown for aero-propulsive effects included and excluded in order to observe the contribution of the discrete and aerodynamic load separately. It can immediately be seen that the aero-propulsive effects have a minor influence on the wing weight. The maximum difference between the two methods is approximately 1%. This suggests that the aerodynamic load on a clean wing can be used in the structural analyses to get a good first approximation. This is a commonly taken approach and is for instance used by Elham et al. [26]. The results are presented in more detail in Figure 18 and the following subsections discuss the effect of the design parameters individually.

1. Clean-wing aerodynamic load assumption

The behaviour shown by the clean aerodynamic wing analysis in Figure 18 is expected and can essentially be explained the bending relief phenomena. A higher shaft power ratio means more power is distributed to the tip engine, increasing its mass which attenuates the wing bending relief. Placing the main engine more outboard will also contribute to this effect. If the main propeller size is increased (and the tip-mounted propeller reduced), the centre of gravity of the propulsion system will move inboard and the bending relief is reduced. Keeping the individual disk loading constant, will lead to a larger engine and a larger propeller size at the tip, for an increase in shaft power ratio. These both increase the weight of the engine at the tip, and eventually reduce the wing mass. In general, any design modification that shifts the centre of gravity of the propulsion system outward will reduce the wing mass when a clean aerodynamic load is assumed. This was also observed by Habermann [12].

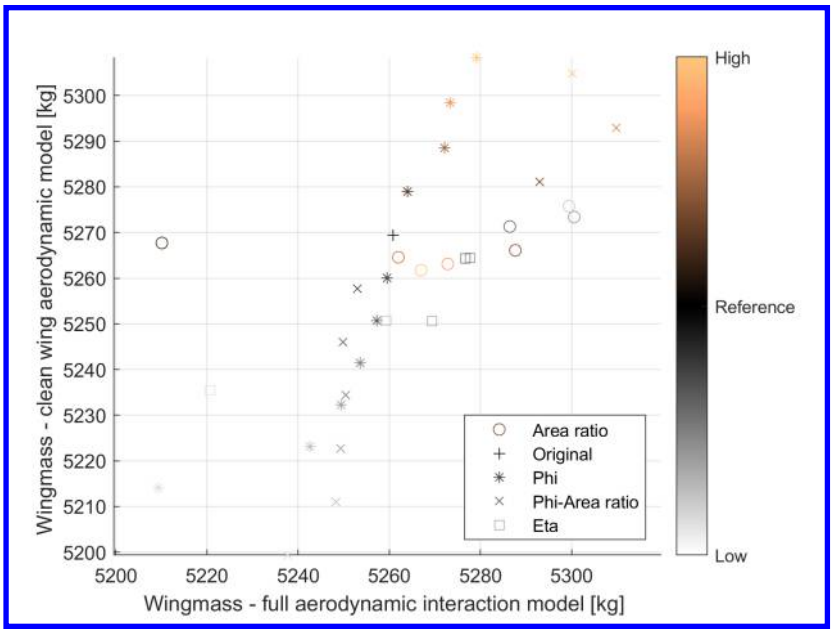

Fig. 17 Overview of wing mass for variable designs.

2. Full aero-propulsive interaction

The effect of the aero-propulsive interaction is not as straight forward. When looking at the effect of the shaft power ratio in Figure 18(a), a negative trend can still be identified; an increased shaft power ratio reduces the wing weight similar to the trend observed for a wing with clean aerodynamic loading assumed. The aero-propulsive effects however, seem to reduce the effect of propulsion system centre of gravity shift. For shaft power ratios below the reference value ($\varphi = 0.2$), the gain in wing mass is less significant compared to the clean-aerodynamic results. Similarly, for shaft power ratios above the reference value, the decrease in wing mass is also less significant. This could explain the observations made by Hoogreef et al. [13] about the potential optimum shaft power ratio. When aero-propulsive effects are included in the structural wing weight estimation, a higher shaft power ratio still shows to be beneficial but the aerodynamic effects weaken the effects of the discrete load.

Figure 18(b) shows that shifting the inboard propeller outboard will help to decrease the wing weight, also when aero-propulsive effects are included. The exact benefit however is expected to be depended on the wing design and taper ratio in particular. If for a tapered wing the propeller is shifted outboard, this will mean that less wing area in immersed in the propeller slipsteam.

The results obtained from sweeping the disk area distribution between main- and tip-propeller are ambiguous as can be seen from Figure 18(c). No clear trend can be identified when aero-propulsive effects are included. Adversely, it suggest that a local minimum exists for the area distribution that minimises the wing mass for a given shaft power ratio. It needs to be emphasised that this optimum may not be the optimum from a purely aerodynamic perspective. However, a difference in wing mass of this order of magnitude can have an impact on the total weight of the aircraft as will be shown in Section V.B.

If the produced power by an engine changes, it seems obvious that the size of the propeller has to change accordingly. That is why the disk area ratio has been coupled to the shaft power ratio. The results are shown in Figure 18(d). For this sensitivity study, the aero-propulsive effects seem to exaggerate the gain in wing mass for low shaft power ratios (φ<0.2). For higher shaft power ratios however, the reduction in wing mass seems to be damped by the aerodynamic effects.

3. Propulsion System Mass

Previous results suggest that a wing weight reduction can be obtained if more power is produced by the secondary shaft. Yet, it should not be disregarded that such a change in propulsive design will also influence the weight of the propulsion system itself. In fact, an increase in shaft power ratio significantly influences the weight of the propulsion system in a negative manner as can be seen in Figure 19. The increase in propulsion system mass is much more significant than the respective decrease in wing mass as was also found by Habermann [12]. The mass penalty introduced by the

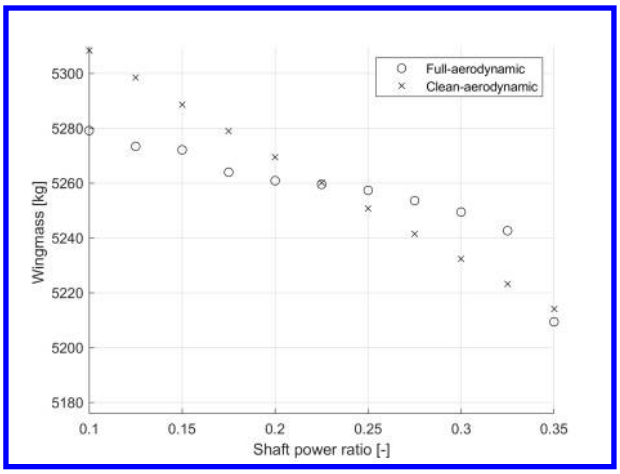

(a) Effect of shaft power ratios.

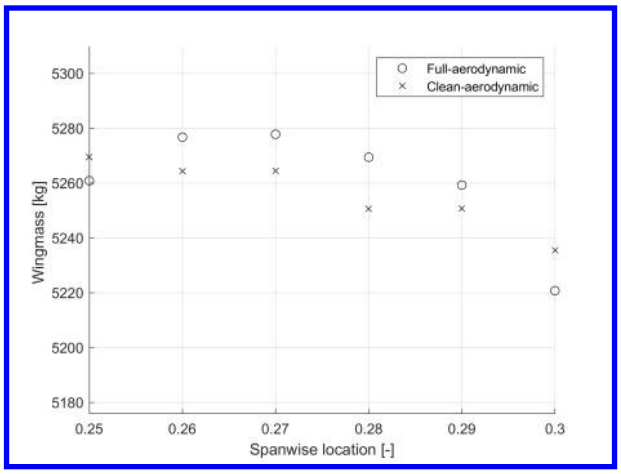

(b) Effect of inboard propeller locations.

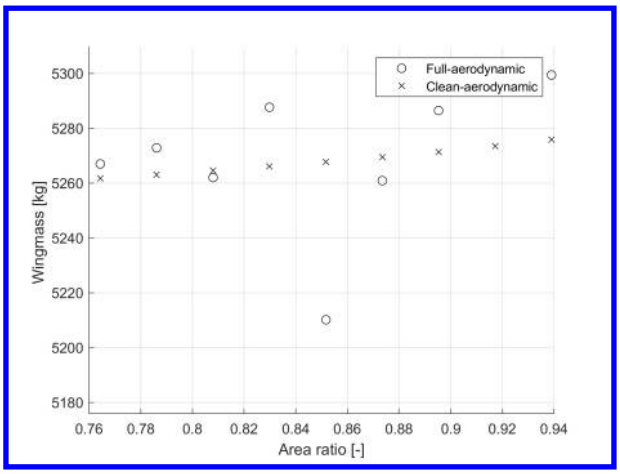

(c) Effect of disk area ratios.

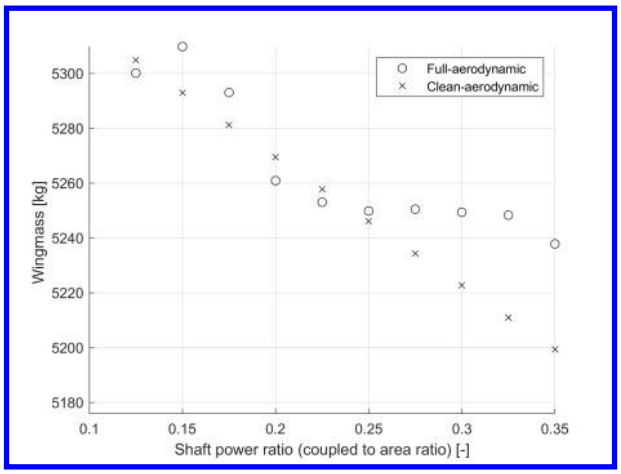

(d) Effect of shaft power ratios with constant individually disk loading.

Fig. 18 Results of sensitivity study on baseline aircraft with $\varphi = 0.2$

turbo-electric propulsion system cannot be compensated by the reduction in wing weight. Within a design convergence it is expected that with increasing shaft power ratio, the wing mass will eventually increase due to a higher weight of the complete wing-propulsive system. This process can potentially be slowed-down by the aerodynamic benefits.

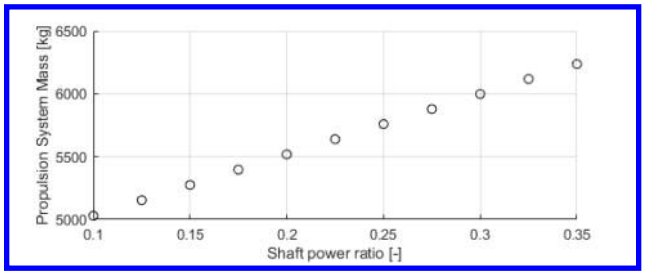

Fig. 19 Effect of shaft power ratio on propulsion system mass.

B. Aircraft Level

As opposed to the study on wing level, the aircraft level sensitivity study does incorporate a feedback loop of the aero-propulsive and aero-structural effects to the overall system as was shown in Figure 12. The effect of the shaft power ratio has been studied in particular. Table 4 shows the different MTOM and wing mass values obtained for the analysis with and without the APS model. It can be seen that a decrease in wing weight is predicted with the APS model included. Although this reduction seems insignificant, it translates into a greater overall reduction and can be noticed in the MTOM. As an example, a reduction of 50 kg leads to reduction of 140kg on MTOM. This suggests that the presented wing weight reductions in Section V.A might have a more significantly impact on aircraft level than sketched before.

Table 4 Effect of shaft power ratio on aircraft mass, with and without aero-propulsive effects on wing aerodynamic loading

	Excluding APS				Including APS			
Shaft power ratio	0.0 (Ref)	0.1	0.2	0.3	0.0 (Ref)	0.1	0.2	0.3
MTOM [tons]	55.86	57.70	59.64	61.95	55.72	57.55	59.32	61.65
Wing mass [tons]	4.84	5.02	5.21	5.42	4.79	4.99	5.18	5.39

1. *Effect of shaft power ratio*

The results concerning the aircraft mass and mass breakdown for the initiated configurations excluding the APS model are shown in Figure 20(a). If the APS effects are not included, a higher shaft power ratio leads to an increase in MTOM. This increase in mass is kick-started by the weight increase of the propulsion system due to a higher shaft power ratio. At first, the wing weight may seem to benefit from a higher shaft power ratio. Yet, the increase in propulsion system weight is much more significant, resulting in a weight increase of the complete system as was also found by Habermann [12]. This, in turn, requires a larger wing and propulsion system to deliver the required lift and power. This again increases the mass further and is a typical snowball effect in aircraft design.

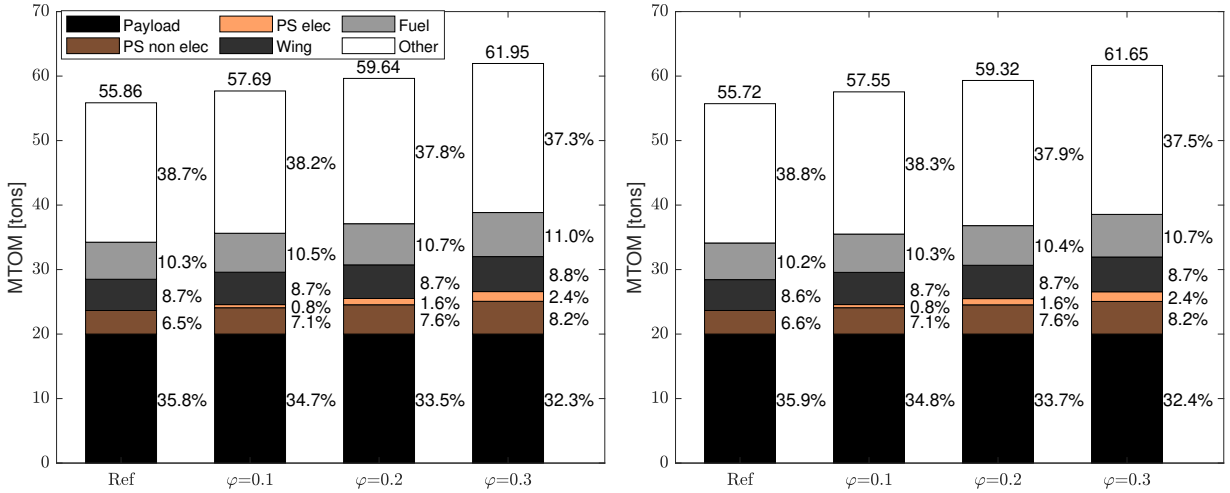

(a) Effect of shaft power ratio on aircraft mass breakdown excluding APS on the wing aerodynamic loading distribution

(b) Effect of shaft power ratio on aircraft mass breakdown including APS on the wing aerodynamic loading distribution.

Fig. 20 Comparison between the effects of shaft power ratio on aircraft mass, with and without aero-propulsive effects on the aerodynamic loading of the wing.

Wingtip-mounted propellers can be used to offer a positive effect on the aerodynamic performance and loading distribution over the wing. However, this effect is overruled by the increase in propulsion system mass. From Figure 20(b), it is clear that the AP and APS effects, are not able to change the direction of the chain reaction. The results do not even suggest that the snowball effect can be reduced by these interaction effects compared to the reference design.

Indeed, as predicted in Section V.A, the effect of the shaft power ratio on the propulsion system is more pronounced for the aircraft level study. This becomes immediately clear from including these results in Figure 19, as is shown in Figure 21. The increase in shaft power ratio will result in approximately the same MTOM increase for both methods as is depicted in Table 5.

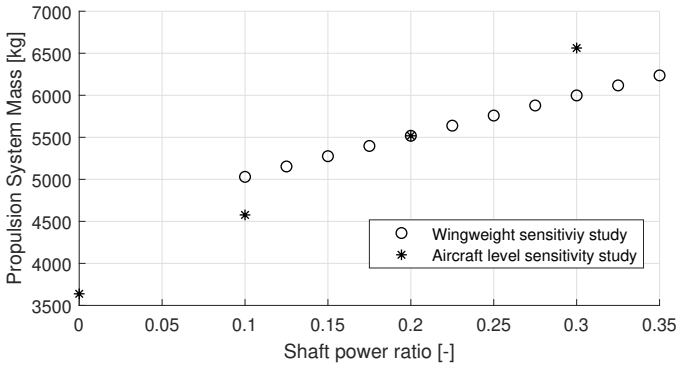

Fig. 21 Propulsion system mass for different shaft power ratios. Wing weight sensitivity results based on φ=0.2 compared to aircraft level results (case study I).

Table 5 MTOM increase compared to reference design

Shaft power ratio	MTOM increase compared to reference design	
	APS excluded	APS included
$\varphi = 0.1$	+3.3%	+3.4%
$\varphi = 0.2$	+6.8%	+6.5%
$\varphi = 0.3$	+10.9%	+10.6%

Overall, the results obtained from the different studies including and excluding the APS model, show similar results. The difference of predicted wing mass is 0.9% at most. For the MTOM this difference is even less (0.4%). The inclusion of the APS effects have a positive influence on the synthesised design in terms of weight. Besides the weight, other parameters can be used to describe the performance of the different designs. A number of these are listed in Table 6. The data is collected from the mission analyses performed in the Class I weight estimation for the cruise phase. The ΔC_L and ΔC_{D_i} indicate the effect of the propulsion on the lift and drag coefficient of the wing compared to a clean configuration as predicted by the aero-propulsive analysis. It can be seen that the induced drag reduces with increasing shaft power ratio at first. At a shaft power ratio of 0.2, both the increase in lift coefficient and reduction in induced drag coefficient are greater than for the conventional reference aircraft. When the shaft power ratio is further increased to 0.3, the lift enhancement and drag reduction both stagnate. This could indicate the location of a local minimum in terms of optimal shaft power ratio for maximum aero-propulsive benefits. This was also suggested by Hoogreef et al. [13]. The propulsive efficiencies are in the expected range. With increasing shaft power ratio, the inboard propeller efficiency slightly increases while the efficiency of the wingtip-mounted propeller slightly decreases. Consequently, the weighted average between the two propulsion chains for their respective power share, η_p, decreases. Moreover, an increase of shaft power ratio has a detrimental effect on the wing aerodynamic efficiency and Payload Range Energy Efficiency (PREE) which is defined as the payload weight times the harmonic range of the aircraft divided by the total energy consumed during the nominal mission and is shown in Equation 3 [22, 27].

$$PREE = \frac{W_{PL}R}{E_{miss}} \tag{3}$$

For the different designs, the isolated wing has a cruise drag coefficient of about 0.033. With the aero-propulsive effects, this induced drag can be reduced by approximately 2%-3% for the presented designs. It seems odd that the reference configuration without a wingtip-mounted propeller attains the highest decrease in induced drag compared to a clean wing. There are various reasons that could explanation this. Most likely, the benefit of wingtip-mounted

Table 6 Effect of shaft power ratio on different performance parameters at cruise conditions (M=0.6), APS included. One lift count = 0.01 and one drag count = 0.0001.

		Shaft power ratio (φ)			
Parameter	Unit	0.0 (Ref)	0.1	0.2	0.3
Lift over drag	-	16.8	16.7	16.9	16.7
ΔC_L	counts	1.4	1.4	2.0	1.8
ΔC_{D_i}	counts	-5.8	-8.9	-10.6	-10.8
η_{ib}	%	85.7	85.9	86.0	86.3
η_{wt}	%	-	86.3	84.8	83.3
η_p	%	85.7	86.3	85.05	84.2
PREE	-	1.65	1.58	1.52	1.42
MTOM	tons	55.7	57.5	59.3	61.6
Wing mass	tons	4.8	5.0	5.2	5.4
Fuel mass	tons	5.7	5.9	6.1	6.6
Span	m	33.4	33.8	34.4	35.1
D_{ib}	m	4.18	4.23	4.29	4.37
D_{wt}	m	-	1.61	1.63	1.67

propellers is not present at low thrust settings, it may even introduce an aerodynamic performance penalty. In this case, it is expected that there is a turning point in shaft power ratio at which the benefit of the wingtip propeller becomes effective. Such a behaviour was also found by Sinnige et al. [4]. Another option is that the wingtip-mounted propeller geometry is non-optimal. As reported by Hoogreef et al. [13] the advance ratio of the tip-mounted system may be constrained by the helicoidal tip Mach number for which the loading distribution assumed here was not optimized for. Therefore, some additional studies into the effects of cruise Mach number and diameter of the wingtip-mounted propellers are presented in the next subsections.

2. Effect of cruise Mach number

The effect of a lower cruising Mach number on the synthesised design has been investigated for different shaft power ratios. Their converged results have been compared to the previously obtained results for Mach 0.6. Figure 22 shows the mass breakdown of the different designs with varying shaft power ratios. When comparing to Figure 20(b), a number of observations can be made. Firstly, decreasing cruise Mach number leads to lighter designs for all φ. In general, a mass reduction in the order of 6-7% is obtained. The higher the shaft power ratio, the higher this reduction (when comparing to a higher cruise speed). At the same time, Table 7 shows that the MTOM seems slightly less sensitive to an increase in shaft power ratio at a lower cruise Mach number. This could indicate that effects of propulsion system mass are less pronounced at lower speed. From the mass breakdown in Figure 22 and 20(b), it can be seen that the mass share of the electric propulsion system components is not effected by the lowered cruise speed. However, the nonelectric components and wing mass show a small decrease in mass contribution.

Performance parameters for the lower speed designs are presented in Table 8. The aero-propulsive interaction benefits from a lower Mach number as the ΔC_L increases and also the induced drag reduction increases compared to the M=0.6 case. This behaviour was expected due to the higher operating lift coefficient of the system. Willemsen [14] showed that higher aero-propulsive benefits can be obtained the higher the operating lift coefficient.

The different designs have an isolated wing cruise drag coefficient of about 0.041. This means that due to the aero-propulsive effects an induced drag reduction of 8%-12% can be obtained. Nevertheless, also a large increase in MTOM is seen of 3%-10%. The combination of the mass gain and aerodynamic benefits results in a decrease of PREE exceeding 11% compared to the conventional reference design.

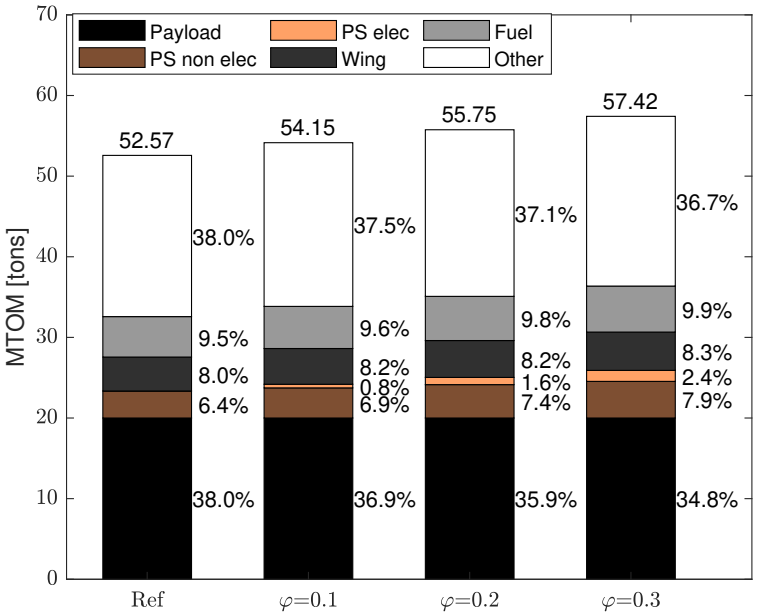

Fig. 22 Mass breakdown for different shaft power ratios for cruise Mach number of 0.5

Table 7 Comparison of MTOM increase with respect to reference design for M=0.5 and M=0.6.

	MTOM compared to reference design; φ=0	
Shaft Power Ratio	M=0.5	M=0.6
φ = 0.1	+3.0%	+3.4%
φ = 0.2	+6.0%	+6.5%
φ = 0.3	+9.2%	+10.6%

3. Effect of propeller diameter

The diameter of the wingtip-mounted propeller has been varied as this affects the disk loading. In the aircraft design process this has been done by varying the span fraction covered by the propulsion system. This has been varied between 10% and 30% wingspan of a design with φ = 0.2.

Considering the aircraft mass breakdown shown in Figure 23, all designs studied show a similar contribution of the different mass components. A slight decreasing contribution of fuel mass is observed. Combined with the overall decreasing MTOM, a distributed propeller fraction of 0.3 yields a fuel reduction of more than 500 kg for the harmonic mission compared to a span fraction of 0.1, which equals almost 10% of the total fuel mass. In conjunction, an increase in PREE is found with increasing tip-mounted propeller diameter. This is due to increasing aero-propulsive benefit with increasing propeller size, causing both lift enhancement and induced drag reduction to increase. Simultaneously, the propulsive efficiency also benefits from a larger propeller, as it is more efficient to accelerate a large amount of air by a small increment compared to a small amount of air by a large increment. When propeller size is increased, disk area increases and disk loading decreases. To deliver a same amount of thrust, the propeller will rotate slower and hence accelerating a larger amount of air by a smaller increment. The increase in propulsive efficiency and wing aerodynamic efficiency result in an increase of PREE (i.e. useful work).

Table 8 Effect of shaft power ratio on different performance parameters at cruise conditions M=0.5, APS included. One lift count = 0.01 and one drag count = 0.0001.

		Shaft power ratio			
Parameter	Unit	0.0 (Ref)	0.1	0.2	0.3
Lift over drag	-	20.75	22.8	22.4	21.9
ΔC_L	counts	2.6	4.5	4.5	4.8
ΔC_{D_i}	counts	-34.3	-59.0	-59.2	-51.0
η_{ib}	%	85.1	85.4	85.6	85.8
η_{wt}	%	-	86.0	84.2	82.6
η_p	%	85.1	85.4	85.3	84.9
PREE	-	1.84	1.80	1.71	1.63
MTOM	tons	52.6	54.1	55.8	57.5
Wing mass	tons	4.2	4.4	4.6	4.7
Fuel mass	tons	5.1	5.2	5.5	5.8
Span	m	32.5	33.0	33.4	33.9
D_{ib}	m	4.00	4.05	4.13	4.15
D_{wt}	m	-	1.57	1.59	1.61

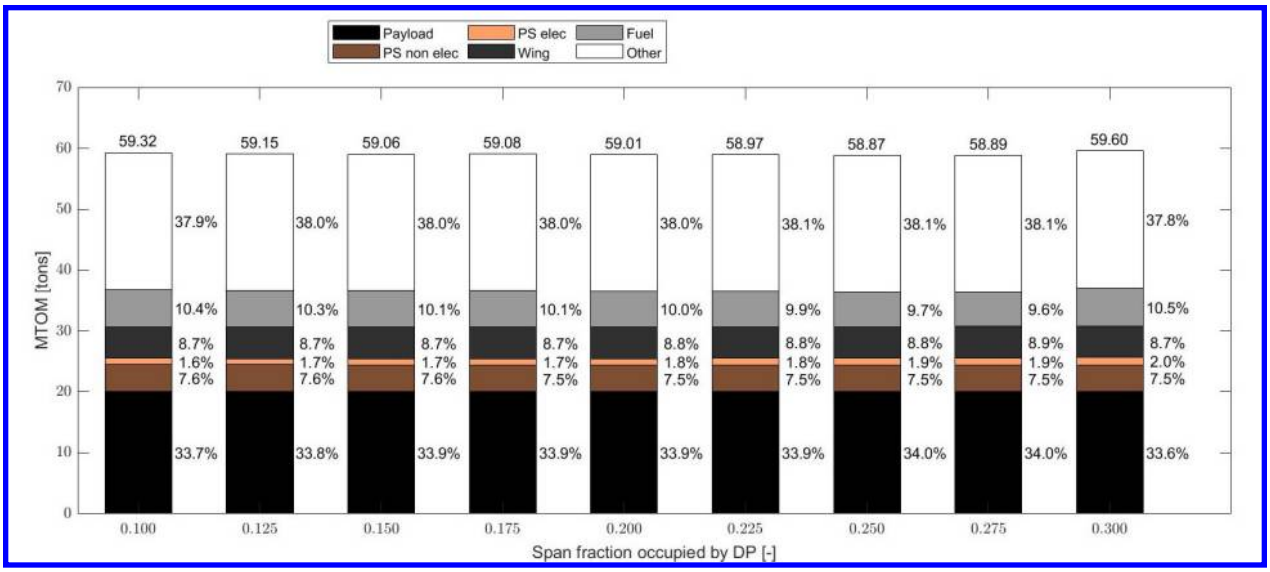

Fig. 23 Mass breakdown for synthesised designs with φ=0.2 and varying wingtip-mounted propeller size.

Table 9 shows that the aerodynamic interaction between propeller and wing seems to benefit from a larger propeller diameter. Both lift enhancement and induced drag reduction are increasing. Similarly, Willemsen [14] that a larger span fraction occupied by the propeller (ΔY) is beneficial in terms of drag since this yields a larger wing area experiencing upwash, decreasing induced drag. The cruise drag coefficient of the isolated wing of the different designs is around 0.033, meaning that an induced drag reduction due to aero-propulsive interaction 3%-16% for the various designs is achieved. Beyond ΔY=0.3 the propulsion system mass again seems to start dominating the design. Yet, more data points need to be gathered to explain the phenomena. Although a performance increase can be observed for increasing wingtip propeller diameter, the mass of the aircraft is still significantly higher than the reference design. Nevertheless, the design with ΔY=0.275 seems to approach the performance as highlighted in Table 9.

Larger tip-mounted propeller diameters result in higher aero-propulsive benefits which at a certain point would be able to negate the mass penalty associated with the PTE configuration. Since this penalty is proportional to the shaft

Table 9 Effect of propeller size on different performance parameters at cruise conditions for φ=0.2, APS included. One lift count = 0.01 and one drag count = 0.0001.

			WTMP span fraction initiated								
Parameter	Unit	Ref	0.100	0.125	0.150	0.175	0.200	0.250	0.225	0.275	0.3
L/D	-	16.8	16.9	17.1	17.3	17.9	18.0	18.9	18.8	19.7	20.3
ΔC_L	counts	1.4	2.0	2.0	2.4	3.0	3.1	3.8	3.6	4.3	4.9
ΔC_{D_i}	counts	-5.8	-11	-14	-17	-23	-23	-35	-35	-45	-52
η_{ib}	%	85.7	86.1	86.1	86.1	86.1	86.1	86.1	86.1	86.1	86.1
η_{wt}	%	-	84.8	85.9	86.5	86.9	87.1	87.3	87.5	87.5	87.6
η_p	%	85.7	85.8	86.0	86.1	86.2	86.3	86.3	86.3	86.4	86.4
PREE	-	1.65	1.52	1.54	1.56	1.56	1.58	1.61	1.63	1.65	1.5
MTOM	tons	55.7	59.3	59.2	59.1	59.1	59.0	59.0	58.9	58.9	59.6
Wing mass	tons	4.8	5.2	5.2	5.2	5.2	5.2	5.2	5.2	5.2	5.2
Fuel mass	tons	5.7	6.1	6.1	6.0	6.0	5.9	5.8	5.7	5.7	6.2
Span	m	33.4	34.4	34.3	34.3	34.3	34.3	34.3	34.3	34.3	34.3
D_{ib}	m	4.18	4.28	4.27	4.27	4.27	4.27	5.27	4.27	4.27	4.25
D_{wt}	m	-	1.63	2.04	2.45	2.86	3.27	3.67	4.08	4.49	4.92

power ratio φ, it is expected for a lower shaft power ratio that the mass penalty can be compensated with a smaller tip-mounted propeller. Hence, the same design sweep was repeated for a shaft power ratio of φ=0.1. The results are shown in Table 10.

Indeed, performance figures of the baseline aircraft can already be matched at smaller occupied span fractions (and consequently smaller diameters); ΔY=0.175-0.200 compared to ΔY=0.275 for φ = 0.2. This confirms that for lower shaft power ratio, it is easier for aero-propulsive interaction benefits to overcome the PTE weight penalty. Moreover, these case studies affirm that the tip-mounted propeller size of the other studies (at span fraction ΔY=0.1) is far from optimal and would require different propeller geometry.

Table 10 Effect of propeller size on different performance parameters at cruise conditions for φ=0.1, APS included. One lift count = 0.01 and one drag count = 0.0001.

			WTMP span fraction initiated								
Parameter	Unit	Ref	0.100	0.125	0.150	0.175	0.200	0.225	0.250	0.275	0.3
L/D	-	16.8	16.7	17.2	17.3	17.9	18.0	18.3	19.1	19.4	19.7
ΔC_L	counts	1.4	1.4	2.0	2.0	2.7	2.8	3.2	3.8	4.0	4.4
ΔC_{D_i}	counts	-5.8	-8	-15	-15	-21	-23	-28	-37	-39	-43
η_{ib}	%	85.7	85.8	85.8	85.8	85.8	85.8	85.8	85.8	85.8	85.8
η_{wt}	%	-	86.3	86.9	87.2	87.4	87.6	87.7	87.7	87.8	87.8
η_p	%	85.7	85.9	85.9	86.0	86.0	86.0	86.0	86.0	86.1	86.1
PREE	-	1.65	1.57	1.59	1.61	1.63	1.67	1.68	1.69	1.73	1.76
MTOM	tons	55.7	57.6	57.5	57.5	57.4	57.3	57.3	57.2	57.2	57.0
Wing mass	tons	4.8	5.0	5.0	5.0	5.0	5.0	5.0	5.0	5.0	5.0
Fuel mass	tons	5.7	5.9	5.9	5.8	5.7	5.6	5.6	5.5	5.4	5.3
Span	m	33.4	33.8	33.8	33.8	33.8	33.8	33.8	33.8	33.8	33.8
D_{ib}	m	4.18	4.23	4.22	4.22	4.22	4.21	4.21	4.21	4.20	4.19
D_{wt}	m	-	1.61	2.01	2.40	2.82	3.22	3.63	4.03	4.43	4.82

VI. Conclusion and directions for future research

Combining the previously presented results, a number of remarks can be made. In general it can be reported that clean wing aerodynamics can be used as a good first estimate for the loading distribution used for the wing weight estimation, as was also found by other researchers. The maximum deviation between the clean aerodynamic wing and full aerodynamic wing studied was in the order of 1%. This confirms that the commonly used assumption of a clean-aerodynamic wing to provide the loading distribution for a wing weight estimation method, is also acceptable in the conceptual design phase of a wingtip-mounted propeller configuration.

Firstly, an increase in shaft power ratio seems to have a positive influence on the wing mass. However, this cannot compensate increase of the propulsion system mass itself. On aircraft level, this results in an increase of MTOM and decrease in aircraft performance. Aero-propulsive and aero-structural benefits gained are easily overshadowed by the weight penalty that is introduced. This is very sensitive to the propeller design (and operating conditions).

Secondly, an almost linear relationship between shaft power ratio and MTOM was observed. For the design with $M_{cr} = 0.6$, an increase from 0.1 to 0.2 φ leads to an increase in MTOM of approximately 3.5% compared to the conventional reference design without wingtip-mounted propulsion. For $M_{cr} = 0.5$, this increment is slightly less (3%).

Thirdly, in terms of MTOM, the increase in propeller size is relatively penalty free when compared to an increase in shaft power ratio while still stimulating the aero-propulsive benefits. When wingtip-mounted propeller diameter is increased, it is eventually possible to attain an equal performance as the conventional reference design in terms of energy efficiency, although facing a mass penalty caused and depend on the shaft power ratio chosen. For $\varphi = 0.1$, the reference performance is attained for a tip-mounted propeller occupied span fraction of $\Delta Y = 0.175$ with an increase in MTOM of 2.8%. For $\varphi = 0.2$, this performance is attained at a larger tip-mounted propeller size (occupied span fraction $\Delta Y = 0.275$) and an increase in MTOM of 5% compared to the reference design.

To further quantify the potential of wingtip-mounted propeller applications, the studies should be repeated with variable wing thickness distribution and a kink in the wing planform to be more representative of actual aircraft wings. Ideally, the aero-propulsive model should be incorporated in more phases of the aircraft design synthesis. Moreover, future studies should include propeller design in the loop to avoid penalizing designs for which the propeller loading is non-optimal. Additionally, further studies on wing-tip mounted propulsion may exploit the propeller usage for stability and control of the aircraft. On the other hand, an engine-inoperative situation might result in a yawing moment that is too large to be corrected by the rudder. Furthermore, noise and aero-elastic phenomena will pose new challenges.

Acknowledgements

This work was partially funded by the European Union Horizon 2020 program, as part of the Clean Sky 2 program for Large Passenger Aircraft (CS2-LPA-GAM-2020/2021-01) under grant agreement No 945583. The authors would like to thank Roger Willemsen for his contributions to the aero-propulsive model, as well as Dr. Tomas Sinnige and Dr. Roelof Vos for their feedback.

References

[1] Kroo, I., "Propeller-wing integration for minimum induced loss," *Journal of Aircraft*, Vol. 23, No. 7, 1986, pp. 561–565. doi:10.2514/3.45344, URL https://doi.org/10.2514/3.45344.

[2] Miranda, L. R., and Brennan, J. E., "Aerodynamic effects of wingtip-mounted propellers and turbines," *4th Applied Aerodynamics Conference*, American Institute of Aeronautics and Astronautics, 1986. doi:10.2514/6.1986-1802, URL https://arc.aiaa.org/doi/abs/10.2514/6.1986-1802.

[3] Snyder, M. H., and Zumwalt, G. W., "Effects of wingtip-mounted propellers on wing lift and induced drag," *Journal of Aircraft*, Vol. 6, No. 5, 1969, pp. 392–397. URL http://arc.aiaa.org/doi/10.2514/3.44076.

[4] Sinnige, T., van Arnhem, N., Stokkermans, T. C. A., Eitelberg, G., and Veldhuis, L. L. M., "Wingtip-Mounted Propellers: Aerodynamic Analysis of Interaction Effects and Comparison with Conventional Layout," *Journal of Aircraft*, Vol. 56, No. 1, 2019, pp. 295–312. doi:10.2514/1.C034978, URL https://doi.org/10.2514/1.C034978.

[5] Veldhuis, L.L.M., "Propeller Wing Aerodynamic Interference," Ph.D. thesis, Delft University of Technology, Jun. 2005. URL http://resolver.tudelft.nl/uuid:8ffbde9c-b483-40de-90e0-97095202fbe3.

[6] Mark D. Moore, "Misconceptions of Electric Aircraft and their Emerging Aviation Markets," *52nd Aerospace Sciences Meeting*, 2014. doi:10.2514/6.2014-0535.

[7] Antcliff, K. R., and Capristan, F. M., "Conceptual Design of the Parallel Electric-Gas Architecture with Synergistic Utilization Scheme (PEGASUS) Concept," *18th AIAA/ISSMO Multidisciplinary Analysis and Optimization Conference*, American Institute of Aeronautics and Astronautics, 2017. doi:10.2514/6.2017-4001.

[8] Blaesser, N. J., "Propeller-Wing Integration on the Parallel Electric-Gas Architecture with Synergistic Utilization Scheme (PEGASUS) Aircraft," *2019 AIAA SciTech Forum and Exposition;*, San Diego, CA, United States, 2019. URL https://ntrs.nasa.gov/search.jsp?R=20200002426.

[9] Borer, N. K., Patterson, M. D., Viken, J. K., Moore, M. D., Bevirt, J., Stoll, A. M., and Gibson, A. R., "Design and Performance of the NASA SCEPTOR Distributed Electric Propulsion Flight Demonstrator," *16th AIAA Aviation Technology, Integration, and Operations Conference*, American Institute of Aeronautics and Astronautics, 2016. doi:10.2514/6.2016-3920.

[10] Cole, J. A., Krebs, T., Barcelos, D., Yeung, A., and Bramesfel, G., "On the Integrated Aerodynamic Design of aPropeller-Wing System," *AIAA Scitech 2019 Forum*, 2019. doi:10.2514/6.2019-2300.

[11] Capristan, M., F., Blaesser, and J., N., "Analysis of the Parallel Electric-Gas Architecture with Synergistic Utilization Scheme (PEGASUS) Concept," Tech. Rep. NASA/TM–2019–220396, L-21042, NF1676-33672, NASA, 2019.

[12] Habermann, A. L., "Effects of Distributed Propulsion on Wing Mass in Aircraft Conceptual Design," *AIAA AVIATION 2020 FORUM*, 2020. doi:10.2514/6.2020-2625.

[13] Hoogreef, M. F. M., de Vries, R., Sinnige, T., and Vos, R., "Synthesis of Aero-Propulsive Interaction Studies Applied to Conceptual Hybrid-Electric Aircraft Design," *AIAA Scitech 2020 Forum*, AIAA, 2020. doi:10.2514/6.2020-0503, URL https://repository.tudelft.nl/islandora/object/uuid%3A2cf180a6-9e0f-417a-af41-45585ea8281d.

[14] Willemsen, R., "A sensitivity studyon the aerodynamicperformance of awingtip-mounted tractorpropeller-wing system," Master's thesis, Delft University of Technology, 2020.

[15] van Arnhem, N., de Vries, R., Sinnige, T., Vos, R., Eitelberg, G., and Veldhuis, L. L. M., "Engineering Method to Estimate the Blade Loading of Propellers in Nonuniform Flow," *AIAA Journal*, 2020, pp. 1–15. doi:10.2514/1.j059485.

[16] Conway, J., "Analytical solutions for the actuator disk with variable radial distribution of load," *Fluid Mechanics*, Vol. 297, 1995. doi:10.1017/s0022112095003120.

[17] Nederlof, R., "Improved modeling of propeller-wing interactions with a lifting-line approach: Investigation of a suitable correction method to account for the finite slipstream height," Master's thesis, Delft University of Technology, 2020. URL https://repository.tudelft.nl/islandora/object/uuid%3Ad952665d-475f-483d-94f5-2b929ea6e713.

[18] Rethorst, S., "Aerodynamic of Nonuniform Flows as Related to an Airfoil Extending Through a Circular Jet"," *Journal of the Aerospace Sciences*, Vol. 25, No. 1, 1958, pp. 11–28. doi:10.2514/8.7479.

[19] Elmendorp, R., and La Rocca, G., "Comparative Deign & Sensitivity Studies on Box-Wing Airplanes," *Italian Association of Aeronautics and Astronautics XXV International Congress 9-12 September 2019*, 2019.

[20] Megson, T. H. G., *Aircraft Structures for Engineering Students.*, Elsevier, 2007.

[21] Torenbeek, E., *Synthesis of Subsonic Airplane Design*, Delft Univ. Press, Delft, The Netherlands, 1982.

[22] de Vries, R., Brown, M., and Vos, R., "Preliminary Sizing Method for Hybrid-Electric Distributed-Propulsion Aircraft," *Journal of Aircraft*, Vol. 56, No. 6, 2019, pp. 2172–2188. doi:10.2514/1.C035388, URL https://arc.aiaa.org/doi/10.2514/1.C035388.

[23] Elmendorp, R. J. M., Vos, R., and La Rocca, G., "A Conceptual Design and Analysis Method for Conventional and Unconventional Airplanes," *ICAS 2014: Proceedings of the 29th Congress of the International Council of the Aeronautical Sciences, St. Petersburg, Russia, 7-12 September 2014*, International Council of Aeronautical Sciences, 2014. URL https://repository.tudelft.nl/islandora/object/uuid%3A1dc55ce5-18c3-4986-b668-f70d9b24aac0.

[24] La Rocca, G., Langen, T., , and Brouwers, Y., "The design and engineering engine. Towards a modular system for collaborative aircraft design," *Proceedings of ICAS 2012*, 2012.

[25] de Vries, R., Hoogreef, M. F. M., and Vos, R., "Aero-Propulsive Efficiency Requirements for Turboelectric Transport Aircraft," *AIAA Scitech 2020 Forum*, American Institute of Aeronautics and Astronautics, 2020. doi:10.2514/6.2020-0502.

[26] Elham, A., La Rocca, G., and van Tooren, M. J. L., "Development and implementation of an advanced, design-sensitive method for wing weight estimation," *Aerospace Science and Technology*, Vol. 29, No. 1, 2013, pp. 100–113. doi:10.1016/j.ast.2013.01.012, URL http://www.sciencedirect.com/science/article/pii/S1270963813000291.

[27] Bijewitz, J., Seitz, A., Isikveren, A. T., and Hornung, M., "Progress in optimizing the propulsive fuselage aircraft concept," *54th AIAA Aerospace Sciences Meeting*, 2016, p. 0767.